sciendo

DOI 10.2478/ama-2024-0004

acta mechanica et automatica, vol.18 no.1 (2024)

AN ADAPTIVE PID CONTROL SYSTEM FOR THE ATTITUDE AND ALTITUDE CONTROL OF A QUADCOPTER

Leszek CEDRO*, Krzysztof WIECZORKOWSKI*, Adam SZCZEŚNIAK*

*Faculty of Mechatronics and Mechanical Engineering, Kielce University of Technology, Aleja Tysiąclecia Państwa Polskiego 7, 25-314 Kielce, Poland

lcedro@tu.kielce.pl, KWieczorkowski@interia.pl, a.szczesniak@tu.kielce.pl

received 25 May 2023, revised 6 September 2023, accepted 12 September 2023

Abstract: In adaptive model-based control systems, determining the appropriate controller gain is a complex and time-consuming task due to noise and external disturbances. Changes in the controller parameters were assumed to be dependent on the quadcopter mass, which was the process variable. A nonlinear model of the plant was used to identify the mass, employing the weighted recursive least squares (WRLS) method for online identification. The identification and control processes involved filtration using differential filters, which provided appropriate derivatives of signals. Proportional integral derivative (PID) controller tuning was performed using the Gauss–Newton optimisation procedure on the plant. Differential filters played a crucial role in all the developed control systems by significantly reducing measurement noise. The results showed that the performance of classical PID controllers can be improved by using differential filters and gain scheduling. The control and identification algorithms were implemented in an National Instruments (NI) myRIO-1900 controller. The nonlinear model of the plant was built based on Newton's equations.

Key words: UAV drone, mechatronics, adaptive control systems

1. INTRODUCTION

The quadrotor has many benefits, such as being highly manoeuvrable, having a small size and simple structure and being able to take off and land vertically. It can also fly at low speeds and stay stationary in the air [1]. However, with six degrees of freedom and only controlled by four inputs, it brings complexity to its position and attitude control [2–4].

A good position and attitude controller are crucial to designing and controlling such a complex system. In control, extensive research has been undertaken for linear and nonlinear control techniques applied to the system. Among them, we find proportional integral derivative (PID) [5–7], linear quadratic regulator (LQR) [8, 9], backstepping control (BC) [10] and sliding mode control (SMC) [11–14]. Controllers (other than PID) are described, for example, in a study mentioned in Ref. [15] (a neural network-based controller). The PID controller is the most commonly used control technique and successfully implemented in the existing system. The PID controller's popularity is due to its simple structure, being easy to design and being easy to tune with satisfactory practical implementation performance [16].

In a study mentioned in Ref. [17], the PID controller with an extended Kalman filter was used to control and stabilise the quadrotor's altitude and attitude angle. The extended Kalman filter was used to filter out the sensor and system noises to stabilise the quadrotor's altitude (3.8 [s]) and attitude angle (5.8 [s]).

A comparative study between PID, proportional derivative (PD) and SMC controllers was conducted [13]. The simulation result showed that the SMC controller has a faster stabilisation time of approximately <3 [s] than PD and PID controllers. Nonetheless, it produces a large pitch and roll angle, making it unfavourable in the real-world condition.

In a study mentioned in Ref. [18], a nonlinear PID-type controller was presented to guarantee the motion control of the quadrotor. The existence of gains was proven by using a Lyapunov-like analysis [19–21], where the quadrotor system's nonlinear dynamics were considered. The authors concluded that the nonlinear PID-type controller they proposed could give better performance than conventional PID and sliding mode controllers since it can provide better tracking accuracy.

A minimal amount of research presents actual experimental results – most of them are simulations only. Outstanding results of aggressive trajectory tracking by a quadcopter have been described in the study mentioned in Ref. [22]. The authors pro-posed a multi-layer control structure: a combination of PD controllers, incremental nonlinear dynamic inversion (INDI) controllers and exploitation of the differential flatness of the quadcopter dynamics. The complete control system tracked the position and yaw angle and their derivatives of up to fourth order, specifically velocity, acceleration, yaw rate and yaw acceleration.

National Instruments (NI) company products, especially their embedded myRIO-1900 devices, are exceptionally well-suited for handling advanced processing tasks needed in complex and demanding applications, including the practical deployment of various flight control systems for unmanned aerial vehicles (UAVs) [23]. With its well-designed architecture and robust onboard features such as a three-axis accelerometer, analogue IO extensions and a Wi-Fi module, the myRIO-1900 platform represents a highly promising embedded solution for the real-world implementation of diverse and intricate flight control systems. Additionally, the associated LabVIEW Real-Time (RT) software tool capitalises on deterministic execution and ensures the highest level of reliability.

The implementation of the developed adaptive procedure was made possible, thanks to the dual-core processor, which, in RT, handled the variable mass identification procedure on one core and the control procedure on the other.

Adaptive controllers are control systems that can adjust their parameters or structure based on changes in the system or environment. The primary goal of adaptive controllers is to maintain system performance and stability under varying operating conditions, such as changes in load, disturbances or system parameters. Adaptive controllers can be divided into two groups: controllers with gain scheduling, where parameters are scheduled using predefined look-up tables, and self-tuning controllers, where parameters are continuously estimated and updated online.

An adaptive control system based on a model is a type of control system that uses a mathematical model of the system being controlled to adjust its parameters in RT. The mathematical model is usually a simplified representation of the plant, which allows for a better understanding of the system's behaviour and can be used to predict how it will respond to changes in the control inputs.

Adaptive control systems have been successfully applied in a wide range of appli-cations, including robotics, aerospace and manufacturing. However, developing an accurate model of the system can be challenging, and the system's performance may be limited by the accuracy of the model.

Gain scheduling refers to a system where the controller parameters depend on the measured operating conditions. Gain scheduling is effective for systems whose dynamics changes with changing operating conditions. Gain scheduling involves modifying the gains of P, I and D terms according to the state of the system. This method works best for systems whose changes in dynamics can be predicted so that the predetermined gains can be calculated and applied. Thus, it is possible to define multiple sets of PID parameters for gain scheduling.

Adaptive control is commonly used to control plants where considerable changes in the operating conditions occur. The variations may be due to disturbances or changes in the plant parameters. One of the ways to handle this problem is to apply continuous adjustment of the control parameters according to the plant parameters. The variable parameter can be measured or assessed by identification [24]. In the case of a quadcopter, the variable parameter is its total mass. The mass of a plant may change when it is used for transport purposes; it will increase when it carries a payload. The mass is an important factor affecting the optimal setpoints of the quadcopter controllers. The control process can be largely improved by employing controllers with gain scheduling. The mass, used as a process variable, can be assessed through online identification; there is no need to employ additional sensors. This approach is easy to implement for any plant, and it is not necessary to change its design.

This study analyses the dynamics of a UAV with four rotors [25], where adaptive controllers are PID controllers with gain scheduling. The identification of the process variable, i.e. drone mass, involved nonlinear parametrisation and differential filtration to obtain appropriate signals and their derivatives.

In this publication, the authors have addressed several key topics:

They developed a method for tuning PID controller parameters specifically tailored for a quadcopter.

They conducted experimental trials to carefully select the parameters of differential filters. This step is crucial to ensure the stable operation of the control system and ac-curate identification of the quadcopter's mass.

The authors also proposed an innovative on-line identification method for determining the quadcopter's mass using differential filters. This method allows for RT mass estimation during flight.

Furthermore, they developed a control system that incorporates gain scheduling, and this system utilises the insights gained from the implementation of differential filters. The gain scheduling aspect ensures that the controller adapts to varying conditions.

Studies in this area have investigated the effectiveness of various control methods, such as LQRs [26, 27], sliding mode controllers [28, 29] and fuzzy logic controllers [30, 31]. The most commonly used type of controllers is PID controllers. Although they are common in quadcopters [32–34], it is still problematic to choose appropriate PID settings. One way to deal with this problem is to optimise the control criteria, e.g. error integral. In this study, the desired setpoints of PID controllers were selected by optimising the integral criterion. All the experiments were carried out for a quadcopter mounted on a test rig, which had four degrees of freedom. The control system was composed of four PID controllers responsible for altitude, roll, pitch and yaw. The control system was built using an NI myRIO-1900 controller and LabVIEW software [35].

2. MATHEMATICAL MODEL OF THE QUADCOPTER DYNAMICS

During mathematical modelling (Fig. 1), physical parameters are described in three different systems, i.e. the Earth system (EF), robot system (local BF) and auxiliary system (SF). The relationship between the EF, BF and SF is shown in Fig. 1b. In the notation of the mathematical model, all physical quantities, except Euler angles, are expressed in the local coordinate system BF. Euler angles are the angles between the system of BF and SF (or EF).

The mathematical model was derived using Newton's equations of motion. The quadcopter (Fig. 1a) is assumed to have six degrees of freedom.

The drone's altitude and attitude q coordinates, represented by the vector (1), consist of six parameters. The first three parameters determine the drone's position in space, while the other three determine its orientation or rotations:

$$\mathrm{q} = [x \quad y \quad z \quad \varphi \quad \theta \quad \psi]^T \tag{1}$$

where x, y, z are position coordinates and φ, θ, ψ are roll, pitch and yaw about the respective coordinate axes.

The first step is to theoretically determine the angular velocity in the local coordinate system, in the same way as that described in a previous study mentioned in Ref. [36]:

$$\Omega = \begin{bmatrix} \omega_x \\ \omega_y \\ \omega_z \end{bmatrix} = \begin{bmatrix} \dot{\varphi} \\ 0 \\ 0 \end{bmatrix} + \mathrm{R}_x \begin{bmatrix} 0 \\ \dot{\theta} \\ 0 \end{bmatrix} + \mathrm{R}_x \mathrm{R}_y \begin{bmatrix} 0 \\ 0 \\ \dot{\psi} \end{bmatrix} \tag{2}$$

where R_x is the rotation matrix for a rotation by the angle φabout the x axis, R_y is the rotation matrix for a rotation by the angle θ about the y axis, R_z is the rotation matrix for a rotation by the angle ψ about the z axis and $\omega_x, \omega_y, \omega_z$are angular velocities in the local coordinate system, which can be written in the following matrix form:

$$\Omega = \mathrm{P}_1 \dot{\Theta} \tag{3}$$

where

$$\mathrm{P}_1 = \begin{bmatrix} 1 & 0 & -\sin\theta \\ 0 & \cos\varphi & \sin\varphi\cos\theta \\ 0 & -\sin\varphi & \cos\varphi\cos\theta \end{bmatrix}, \ \dot{\Theta} = \begin{bmatrix} \dot{\varphi} \\ \dot{\theta} \\ \dot{\psi} \end{bmatrix} \tag{4}$$

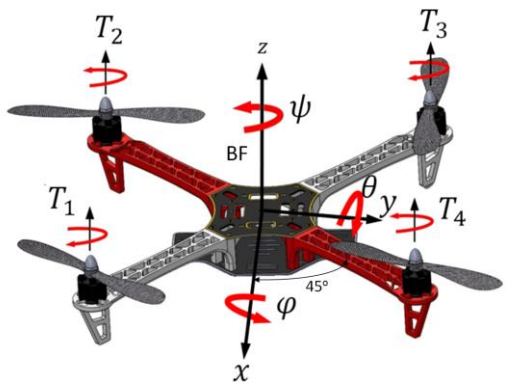

(a)

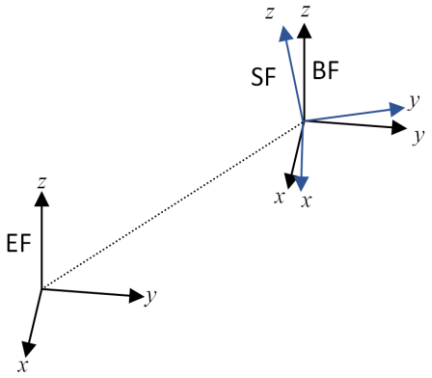

(b)

Fig. 1. Quadcopter (a) and modelling systems (b)

The next step is to calculate the inverse of the matrix P_1

$$\mathrm{P}_2 = (\mathrm{P}_1)^{-1} = \begin{bmatrix} 1 & \sin\varphi\tan\theta & \cos\varphi\tan\theta \\ 0 & \cos\varphi & -\sin\varphi \\ 0 & \sin\varphi\sec\theta & \cos\varphi\sec\theta \end{bmatrix} \tag{5}$$

Finally, knowing the matrix P_2, which is dependent on the angular velocity of the auxiliary coordinate system, we can define the Euler rates as follows:

$$\dot{\Theta} = \mathrm{P}_2\Omega \tag{6}$$

The next step is to define the linear acceleration using Newton's second law of motion. The general form equation for linear acceleration can be expressed using vectors:

$$m\mathrm{a} = \mathrm{F} - \mathrm{F}_g - \mathrm{F}_{Co} - \mathrm{F}_{Cw} \tag{7}$$

where m is the quadcopter mass, a is the linear acceleration matrix, F is the sum of thrusts produced by all the motors, F_g is the gravitational force, F_{Co} are Coriolis forces resulting from the quadcopter rotations and F_{Cw} are Coriolis forces resulting from the rotors rotations.

As can be seen from Eq. (7), the constraint is the force decreased by the gravitational force and the Coriolis forces. The gravitational force Eq. (8) can be defined as a force projected from the local coordinate system to the auxiliary system. The gravitational acceleration g is thus multiplied by the total mass of the quadcopter and the rotation matrixP_2:

$$\mathrm{F}_g = \mathrm{P}_2\, m \begin{bmatrix} 0 \\ 0 \\ g \end{bmatrix} = \begin{bmatrix} -mg\sin\theta \\ mg\sin\varphi\cos\theta \\ mg\cos\varphi\cos\theta \end{bmatrix} \tag{8}$$

The first of the Coriolis forces results from the rotation of the entire quadcopter:

$$\mathrm{F}_{Co} = 2m\ \Omega \times \mathrm{v} = 2m \begin{bmatrix} v_z\omega_y - v_y\omega_z \\ v_x\omega_z - v_z\omega_x \\ v_y\omega_x - v_x\omega_y \end{bmatrix} \tag{9}$$

where vis the linear velocity matrix and v_x, v_y,v_z are linear velocities in the local coordinate system.

The second of the Coriolis forces results from the rotations of the rotors:

$$\mathrm{F}_{Cw} = 2m_w\Omega_w \times \mathrm{v} = 2m_w \begin{bmatrix} -v_y(\omega_1 + \omega_2 + \omega_3 + \omega_4) \\ v_x(\omega_1 + \omega_2 + \omega_3 + \omega_4) \\ 0 \end{bmatrix} \tag{10}$$

where the sum of rotors angular velocity matrix Ω_w can be expressed as follows:

$$\Omega_w = \begin{bmatrix} 0 \\ 0 \\ \omega_1 + \omega_2 + \omega_3 + \omega_4 \end{bmatrix} \tag{11}$$

Where ω_i is the angular velocity of the i-th motor.

The lift F, being the sum of thrusts produced by all the motors, is generated vertically upwards along the drone's vertical axis Z; it is described by the following formula (12):

$$\mathrm{F} = \begin{bmatrix} 0 \\ 0 \\ F_z \end{bmatrix} = \begin{bmatrix} 0 \\ 0 \\ T_1 + T_2 + T_3 + T_4 \end{bmatrix} \tag{12}$$

where F is the vector of sum of thrust of all motors and T_i is the thrust force of the i-th motor.

The next step is to calculate angular acceleration. This effect can be described mathematically using Euler's equation of rigid-body motion. The general vector form of Euler's equation can be written as follows:

$$\tau = \frac{d\mathrm{L}}{dt} + \Omega \times \mathrm{L} \tag{13}$$

where L is the angular momentum and τ is the thrust moment.

It is also true that for a rigid body,

$$\mathrm{L} = \mathrm{I}\,\Omega \tag{14}$$

where I is described by the following matrix:

$$\mathrm{I} = \begin{bmatrix} J_x & 0 & 0 \\ 0 & J_y & 0 \\ 0 & 0 & J_z \end{bmatrix} \tag{15}$$

where $\mathrm{J_x}$, $\mathrm{J_y}$, $\mathrm{J_z}$ are moments of inertia about the respective coordinate axes.

The inertia matrix I for the quadcopter can be diagonalised in a matrix transform due to the symmetry of the quadcopter's geometry. Therefore, the inertia matrix I is assumed to be expressed in Eq. (15) during the derivation.

Thus, substituting Eq. (13) into Eq. (14) and assuming that the moment of inertia is constant, we have the following expression:

$$\tau = \mathrm{I}\,\dot{\Omega} + \Omega \times (\mathrm{I}\,\Omega) \tag{16}$$

DOI 10.2478/ama-2024-0004

Eq. (16) needs to be adjusted because the motors and rotors cause the gyroscopic effect [37, 38]. This effect is described by the fundamental equation of the gyroscope:

$$\tau_{gyro} = \Omega \times \mathrm{L}_p \tag{17}$$

The angular momentum vectorL_p is determined by multiplying the moment of inertia of the rotor (I_w) by the rotor's angular velocity in the axis where the rotation occurs (Ω_w):

$$\mathrm{L}_p = I_w\,\Omega_w = \begin{bmatrix} 0 \\ 0 \\ I_w\,(\omega_1 + \omega_2 + \omega_3 + \omega_4) \end{bmatrix} \tag{18}$$

Knowing L_p and Ω, we can expand Eq. (17) as follows:

$$\tau_{gyro} = \begin{bmatrix} \omega_x \\ \omega_y \\ \omega_z \end{bmatrix} \times \begin{bmatrix} 0 \\ 0 \\ I_w\,(\omega_1 + \omega_2 + \omega_3 + \omega_4) \end{bmatrix} = \\ = \begin{bmatrix} \omega_y I_w(\omega_1 + \omega_2 + \omega_3 + \omega_4) \\ -\omega_x I_w(\omega_1 + \omega_2 + \omega_3 + \omega_4) \\ 0 \end{bmatrix} \tag{19}$$

With the gyroscopic torque being in the vector form, Euler's Eq. (13) can be upgraded and described by using the following formula:

$$\tau = \mathrm{I}\dot{\Omega} + \Omega \times (\mathrm{I}\Omega) + \tau_{gyro} \tag{20}$$

In Eq. (20), the unknown quantity is the angular acceleration; thus, after transformations, it can be written as follows:

$$\dot{\Omega} = \mathrm{I}^{-1}(\tau - \Omega \times (\mathrm{I}\Omega) - \tau_{gyro}) \tag{21}$$

For the configuration coordinates responsible for the rotations φ, θ and ψ, the thrust moments τ are expressed in the form of moments M_φ, M_θ and M_ψ, Eqs. (22–24), respectively:

$$M_\varphi = (-T_1 - T_2 + T_3 + T_4)\,\frac{l}{\sqrt{2}} \tag{22}$$

$$M_\theta = (-T_1 + T_2 + T_3 - T_4)\,\frac{l}{\sqrt{2}} \tag{23}$$

$$M_\psi = \sum_{i=1}^{4} M_i \tag{24}$$

where l is the distance between the i-th motor and the centre of gravity of the drone.

Equations (22–24) demonstrate that the ability of the quadcopter to be controlled is influenced by the thrust force generated in the z direction F_z as well as the rotational moments M_φ, M_θ and M_ψ. The thrust of the i-th motor T_i is determined by calculating the square of the angular velocity of the i-th rotor and multiplying it by a gain correction factor b:

$$T_i = b\omega_i^2 \tag{25}$$

The moment on the i-th motor shaft Mi can be calculated from the angular velocity of the i-th rotor Eq. (26):

$$M_i = d\omega_i^2 \tag{26}$$

where b, d are correction factors.

The axes of the body coordinate system do not coincide with the quadcopter rotor arms and are rotated by the $\frac{\pi}{4}$ angle around the body z axis (Fig. 1). After substituting Eqs (25) and (26) into Eqs (22–24) and multiplying them by the rotation matrix for the$\frac{\pi}{4}$angle, we obtain

$$\tau = \begin{bmatrix} M_\varphi \\ M_\theta \\ M_\psi \end{bmatrix} = \begin{bmatrix} \frac{lb(-\omega_1^2 - \omega_2^2 + \omega_3^2 + \omega_4^2)}{\sqrt{2}} \\ \frac{lb(-\omega_1^2 + \omega_2^2 + \omega_3^2 - \omega_4^2)}{\sqrt{2}} \\ d(\omega_1^2 - \omega_2^2 + \omega_3^2 - \omega_4^2) \end{bmatrix} \tag{27}$$

Knowing the other terms and forces, we can write the model of the quadcopter in the following way. The first part of the model refers to linear acceleration, which is defined in the local coordinate system:

$$\mathrm{a} = \begin{bmatrix} \ddot{x} \\ \ddot{y} \\ \ddot{z} \end{bmatrix} = \begin{bmatrix} 0 \\ 0 \\ \frac{b}{m}(\omega_1^2 + \omega_2^2 + \omega_3^2 + \omega_4^2) \end{bmatrix} - \begin{bmatrix} -g\sin\theta \\ g\sin\varphi\cos\theta \\ g\cos\varphi\cos\theta \end{bmatrix} + \\ -2\begin{bmatrix} v_z\omega_y - v_y\omega_z \\ v_x\omega_z - v_z\omega_x \\ v_y\omega_x - v_x\omega_y \end{bmatrix} - 2\,\frac{m_w}{m}\begin{bmatrix} -v_y(\omega_1 + \omega_2 + \omega_3 + \omega_4) \\ v_x(\omega_1 + \omega_2 + \omega_3 + \omega_4) \\ 0 \end{bmatrix} \tag{28}$$

where $\mathrm{m_w}$ is the mass of propellers and rotors.

The second part represents Euler rates, which will be used to determine changes in the orientation of the quadcopter local system in relation to that of the auxiliary system:

$$\dot{\Theta} = \begin{bmatrix} \dot{\varphi} \\ \dot{\theta} \\ \dot{\psi} \end{bmatrix} = \begin{bmatrix} \omega_x + \omega_y\sin\varphi\,\tan\theta + \omega_z\cos\varphi\,\tan\theta \\ \omega_y\cos\varphi - \omega_z\sin\varphi \\ \omega_y\sin\varphi\sec\theta + \omega_z\cos\varphi\sec\theta \end{bmatrix} \tag{29}$$

The last part is directly related to angular accelerations:

$$\dot{\Omega} = \begin{bmatrix} \dot{\omega}_x \\ \dot{\omega}_y \\ \dot{\omega}_z \end{bmatrix} = \begin{bmatrix} \frac{lb}{J_x\sqrt{2}}(-\omega_1^2 - \omega_2^2 + \omega_3^2 + \omega_4^2) \\ \frac{lb}{J_y\sqrt{2}}(-\omega_1^2 + \omega_2^2 + \omega_3^2 - \omega_4^2) \\ \frac{d}{J_x}(\omega_1^2 - \omega_2^2 + \omega_3^2 - \omega_4^2) \end{bmatrix} + \\ -\begin{bmatrix} \frac{1}{J_x}\left(\omega_y\omega_z(J_z - J_y)\right) \\ \frac{1}{J_y}\left(\omega_x\omega_z(J_x - J_z)\right) \\ \frac{1}{J_z}\left(\omega_x\omega_y(J_y - J_x)\right) \end{bmatrix} + \\ -\begin{bmatrix} \frac{1}{J_x}\left(\omega_y I_w(\omega_1 + \omega_2 + \omega_3 + \omega_4)\right) \\ \frac{1}{J_y}\left(-\omega_x I_w(\omega_1 + \omega_2 + \omega_3 + \omega_4)\right) \\ 0 \end{bmatrix} \tag{30}$$

The relationships between the angular velocities$\omega_\mathrm{i}$of the motors and the respective control signals $\mathrm{U_i}$ are given as follows:

$$\begin{bmatrix} U_1 \\ U_2 \\ U_3 \\ U_4 \end{bmatrix} = \begin{bmatrix} b & b & b & b \\ -\frac{bl}{\sqrt{2}} & 0 & \frac{bl}{\sqrt{2}} & 0 \\ 0 & \frac{bl}{\sqrt{2}} & 0 & -\frac{bl}{\sqrt{2}} \\ d & -d & d & -d \end{bmatrix} \begin{bmatrix} \omega_1^2 \\ \omega_2^2 \\ \omega_3^2 \\ \omega_4^2 \end{bmatrix} \tag{31}$$

$$\mathbf{U} = [U_1 \quad U_2 \quad U_3 \quad U_4]^T$$

3. IDENTIFICATION METHOD

One of the most popular and effective methods of identification is the least squares (LS) method, which is based on the processing of input and output signals [39].

High-quality control under static and dynamic conditions can be achieved using microchip-based methods. However, these

require precise information on the actual values of the parameters of the mathematical model of the system [40–44].

In this study, specially developed low-pass filters and low-pass differentiating filters were employed to filter inputs and outputs to obtain signals and their derivatives required in the identification process.

Since the proposed control method involves identifying one parameter, i.e. the quadcopter mass, the formulae to describe this case will be provided further in this article. Consider a model as follows:

$$\mathrm{v_k} = \mathrm{w_k p} \tag{32}$$

where p is the unknown parameter, $\mathrm{v_k}$and $\mathrm{w_k}$ are scalar signals and $\mathrm{k} = 0, 1, \ldots$ are successive time instants.

The LS algorithm uses plant variables that were recorded over a long enough period of time interval $\mathrm{k} = 0, 1, \ldots, \mathrm{N} - 1$.

This approach is known as the recursive LS algorithm with exponential forgetting or the weighted recursive least squares (WRLS) algorithm [45].

The WRLS algorithm minimises an objective function by exponentially forgetting older data

$$J_k(p) = \sum_{i=1}^{k} \lambda^{k-i}(v_i - w_k p)^2 \tag{33}$$

with respect to the parameter p, where λ is a constant satisfying the inequality $0 < \lambda < 1$. Let $\hat{\mathrm{p}}_\mathrm{k}$ represent a value of the parameter p for which $\mathrm{dJ_k(p)/dp} = 0$. Using a simple transformation, we get

$$\hat{p}_k = \hat{p}_{k-1} + \gamma_k w_k (v_k - w_k^T \hat{p}_{k-1}) \tag{34}$$

$$\gamma_k^{-1} = \lambda \gamma_{k-1}^{-1} + w_k^2, k = 1,2,\ldots \tag{35}$$

In criterion Eq. (33), the components dependent on the past measurement data are multiplied by the factor $\lambda^{\mathrm{k-i}}$. This implies that when the estimate of p is determined, the past measurement data are less important than the present data. The parameter λ is called a forgetting factor.

Suppose that the plant equation satisfies relationship Eq. (32) depending on the plant input and output [45].

It is assumed that parameter estimates will be updated immediately after a certain number of signal samples$\mathrm{N}$. The aim is to derive a recursive equation for determining parameter estimates $\mathrm{p_m}$ for the time instants lying in the interval $\alpha(\mathrm{m}) = [(\mathrm{m}-1) \cdot \mathrm{N}, \mathrm{m} \cdot \mathrm{N} - 1], \mathrm{m} = 1,2,\ldots$.

Define the following objective function:

$$J_m(p) = \sum_{j=1}^{m} \lambda^{m-j}\left(v_i - w_k p_j\right) \tag{36}$$

$$\hat{p}_m = \hat{p}_{m-1} + \gamma_m \sum_{i \in \alpha(m-1)} w_i (v_i - w_i \hat{p}_{m-1}) \tag{37}$$

$$\gamma_m^{-1} = \lambda \gamma_{m-1}^{-1} + \sum_{i \in \alpha(m-1)} w_i^2, m = 1,2,\ldots \tag{38}$$

Generally, it is assumed that $\gamma_0^{-1} = \varepsilon$ for ε ranging $10^3 - 10^6$. Small initial values of the scalarγ_0^{-1} ensure immediate convergence of the estimates to the real values of the parameters at the beginning of the algorithm.

4. SELECTING THE SETPOINTS FOR PID CONTROLLERS

The usual method to adjust the parameters of a controller is through a trial and error method, but this process can be time-consuming and tiresome. It is essential to tune the controller's parameters properly to get optimal performance, but the traditional way may not always provide the best solution.

Furthermore, the control designer can never tell which exact parameters are the optimal solution for the controller [46]. To overcome the issue of the tedious trial and error method of tuning controller parameters, many researchers have started using optimisation tools in their work to find the optimal values of the controller parameters easily.

The advantages of these optimisations are that they are independent problem structures [47]. Different algorithms have been used to obtain the optimal parameters of the controllers. Among them, we can find the genetic algorithm (GA) [48], ant colony optimisation (ACO) [49], artificial bee colony (ABC) [50] and cuckoo search (CS) [51, 52].

In their research study, Imane and Mostafa investigated how to optimise the gain parameter of a PID controller for altitude and attitude angle control of a quadrotor [53]. They used two optimisation methods, RM and GA, to obtain the optimal gain parameter.

Erkol [47] conducted a study on the optimal tuning of PID control for attitude and hover control of the quadrotor. The study used various optimisation techniques, including ABC, particle swarm optimisation (PSO), GA and the Ziegler–Nichols method. The findings indicate that controllers based on ABC and GA perform the best in terms of integral absolute error (IAE) and root mean square error (RMSE), while the ZN method results in the worst performance.

Tuning the PID controllers responsible for the quadcopter control requires selecting their setpoints: $\mathrm{K_{Pi}}$, $\mathrm{K_{Ii}}$ and$\mathrm{K_{Di}}$. From Eq. (39), it is clear that the number of parameters sought can be reduced from 12 to 9. Because of the drone symmetry, it can be assumed that the drone can be rotated by the φangle around the body x axis and by the θangle around the body y axis by using PID controllers with the same setpoints. As the quadcopter mounted on the test rig has a limited number of degrees of freedom, the q vector is defined as follows:
$\mathrm{q} = [z \quad \varphi \quad \theta \quad \psi]^T$. Thus,

$$U_i = K_{Pi} e_i + K_{Ii} \int e_i(\tau) d\tau + K_{Di} \dot{e}_i, i = 1,2,3,4 \tag{39}$$

$$e_1 = z_z - z, e_2 = \varphi_z - \varphi, e_3 = \theta_z - \theta, e_4 = \psi_z - \psi \tag{40}$$

$$\mathrm{q_z} = [z_z \quad \varphi_z \quad \theta_z \quad \psi_z]^T, \mathrm{e} = [e_1 \quad e_2 \quad e_3 \quad e_4]^T$$

where
z_z, φ_z, θ_z and ψ_z are setpoints.

The choice of the best PID parameters is dependent on various factors, including the dynamic response of the plant, as well as on the control objectives determined by the operator. The selection task can be difficult and time-consuming when the controller setpoints are set manually and software is used to optimise the PID parameters. The methods that do not require creating a mathematical model include autotuning employed in controllers with automatic setpoint selection. However, automatic setpoint selection systems may not be able to handle the measurement noise, which in the case of a quadcopter is considerable. In this study, the tests of automatic tuning of PID setpoints for the drone were not repeatable, and the desired level of confidence was not reached. High levels of measurement noise affected the estimates of the process variable.

Because of the nonlinearity of the plant, i.e. a quadcopter with multiple input and multiple output (MIMO), and high levels of measurement noise generated by the quadcopter, the number of setpoint selection methods that can be used is limited. In this case, setpoint selection generally involves optimising the control criteria (integral criteria); it does not require a mathematical model.

DOI 10.2478/ama-2024-0004

The diagram in Fig. 2 shows the optimisation of the setpoints of the PID controllers achieved by employing a minimisation algorithm. The Gauss–Newton algorithm [54] is used to minimise the target function $J = \int \frac{1}{2} \|e\|^2 \, d\tau$.

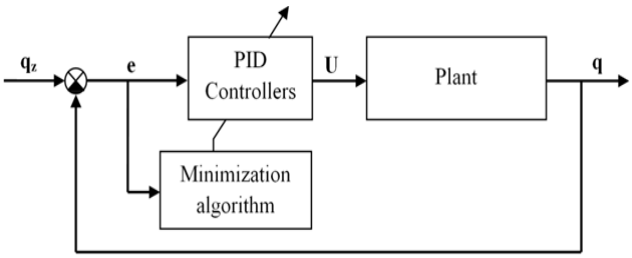

Fig. 2. Diagram of the optimisation of the PID controller setpoints. PID, proportional integral derivative.

The optimisation of the setpoints was performed in LabVIEW for the plant shown in Fig. 3. An MPU-6050 sensor was employed to measure angular positions in three axes. The height z that the quadcopter reached was measured using a linear variable differential transducer (LVDT). The quadcopter is equipped with MT2216 II 810KV brushless motors CW CCW with 1045 propellers. The range of the quadcopter's tested mass is 1.65-2.0 kg, and the allowable change in altitude is within the range of 0–0.15 m. The test setup is powered by a voltage of 12 V provided by two power supplies (62A each).

Fig. 3. Test rig with the quadcopter

To work correctly, the minimisation algorithm requires determining the initial values of setpoints and their ranges. The optimisation procedure performed for nine parameters can be much easier if the range is defined based on the simulation data and a priori knowledge. Ultimately, the setpoints of the PID controllers were estimated for three mass values, which will be the basis to calculate the final values of the setpoints for the mass identified using the adaptive algorithm (Tab. 1).

Tab. 1. PID gains obtained using the optimisation procedure

m [kg]	PID controllers	K_P	K_I	K_D
1.65	1	0.4200	0.01360	0.3999
	2 and 3	0.0700	0.00990	0.0200
	4	0.0300	0.00009	0.0219
1.72	1	0.5249	0.02835	0.4000
	2 and 3	0.0700	0.00999	0.0200
	4	0.0299	0.00099	0.0220
1.79	1	0.6300	0.03255	0.4000
	2 and 3	0.0700	0.01000	0.0200
	4	0.0400	0.00100	0.0200

PID, proportional integral derivative

To check the stability of drone control, various methods and tools can be used. One of the most commonly used methods is analysing the step or impulse response of the drone to the given control signals. This involves introducing a sudden change in the control signal and then observing how the drone reacts and how quickly it achieves stability. Another method is to examine the dynamic characteristics of the drone, such as speed, acceleration and rotation angles, depending on the control signals. For drones, an important factor for stability is height control, which can be checked by observing the drone's behaviour during maintaining constant altitude or during takeoff and landing. For more advanced drone control systems, computer simulations can also be used to test the system's performance in various conditions and scenarios.

The proposed drone control systems in this article were tested for stability at different operating points. The observation of the drone's dynamics and maintaining a constant altitude confirmed the stability of the developed control systems for the settings presented in Tab. 1 and the intermediate settings resulting from their linear interpolation.

5. ADAPTIVE ATTITUDE AND ALTITUDE CONTROL SYSTEM

This article presents a simpler solution using gain scheduling adaptive control systems. The experiments were conducted under laboratory conditions.

For the analysed plant, the setpoints of the controllers were adjusted depending on the change in the drone mass, which is the process variable (Fig. 4). The setpoints of the controllers for intermediate mass are determined from the linear interpolation between the basic setpoints given in Tab. 1.

The drone mass was estimated by identification, which involved using a WRLS algorithm and derivatives of signals, obtained by means of differential filtration [55].

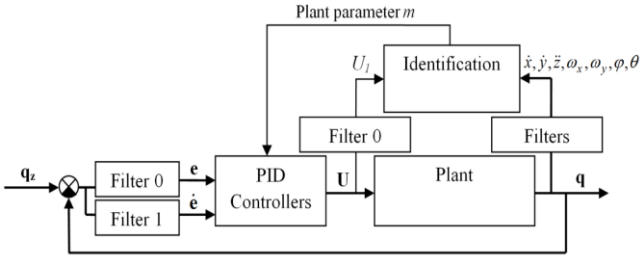

Fig. 4. Adaptive control system PID, proportional integral derivative

In the diagram given in Fig. 4, the Filters block contains three filters that perform low-pass filtering and first- and second-order differentiation. The PID Controllers block includes a set of parameters (Tab. 1) and performs linear interpolation based on the leading variable m. Linear interpolation of PID controller parameters is only possible within the provided set of parameters (Tab. 1). To limit measurement noise for individual signals, low-pass filters are implemented in the Filter 0 blocks. The Filter 1 block contains a differentiating filter that simultaneously calculates signal derivatives and reduces measurement noise.

The identification process uses Eq. (41), where the mass is estimated using the WRLS procedure:

$$U_1 = m\ddot{z} + mg\cos(\theta)\cos(\varphi) + 2m(\omega_x\dot{y} - \omega_y\dot{x}) \quad (41)$$

The next step involves parametrising the model Eq. (41) to ensure accurate identification. The parameter of the model can be determined as follows:

$$p = m, g = 9.81 \quad (42)$$

With a given parameter determined in this way, Eq. (41) takes the following form:

$$U_1 = p\,\ddot{z} + p\,9.81\cos(\theta)\cos(\varphi) + 2p(\omega_x\dot{y} - \omega_y\dot{x}) \quad (43)$$

As can be seen, Eq. (43) is linear with respect to the parameter$p$. Using Eq. 43, we obtain

$$v = w\,p \quad (44)$$

where

$v = \ U_1, w = \ddot{z} + 9.81\cos(\theta)\cos(\varphi) + 2(\omega_x\dot{y} - \omega_y\dot{x})$.

The parameter estimates are updated every N = 129 samples at $\Delta = 0.004$s. The identification process required preparing special derivatives of signals and eliminating most of the measurement noise. The advantage of the differential filters is that they ensure good estimation of the derivatives of signals and also help reduce the measurement noise [56]. In this study, differential filters were used not only in the identification procedure but also to assess e and ė signals. The test results suggest a considerable improvement in the control process, where eandėsignals were obtained through filtration using a low-pass filter (Filter 0) and a differential filter (Filter 1) (Tab. 2). The use of the filters in the control algorithm required selecting the right parameters to ensure a small delay as well as good estimation of signals and their derivatives. The experimentally selected parameters of the filters used in the PID algorithm were as follows: boundary frequency $\Omega_g = 0.08$[rad/s] and total bandwidth of FIR filters$2 \cdot$ ters$2 \cdot M_f + 1 = 7$.

The procedure to identify the quadcopter mass at a sudden change in mass (29 [s], m + 70 g) is accurate, taking only several seconds (Fig. 5).

The initial mass identification outliers resulted from the quadcopter lift off the ground ($z = 0\ [m]$) and high initial values of the matrixγ_0^{-1}.Very good results were obtained when the WRLS algorithm governed by the forgetting factor$\lambda = 0.98$ was applied. The value of this factor has a considerable influence on the rate at which the procedure responds to a change in the actual mass. The high value of this factor is responsible for slow changes in the mass and high precision in the determination of its value, which has a beneficial effect on the control stability. The NI myRIO-1900 controller, with low computational capacity, was responsible for controlling the quadcopter and estimating its mass. The WRLS identification procedure was initiated every 2 Hz. This frequency (used to determine the mass) was optimal for the controller, and it allowed us to collect the right amount of data to ensure the stability of the WRLS procedure. As the stability of the mass identification procedure is essential, the signals and their derivatives were estimated with high precision. Thus, the filters used in this procedure had settings different from the filters employed in the PID control algorithm. The best results were reported for the following filter parameters: $\Omega_g = 0.2$[rad/s] boundary frequency and the total bandwidth of the FIR filters being $2 \cdot M_f + 1 = 129$.

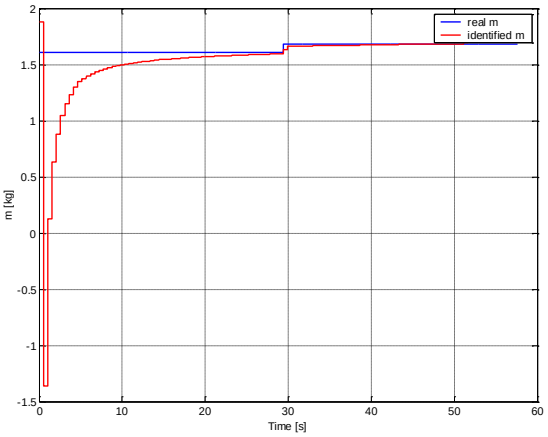

Fig. 5. Identification of the quadcopter mass

From Tab. 2, it is clear that the control output values obtained for PID controllers with gain scheduling (adaptive PID controllers) are better than those reported for PID controllers with fixed gains, which ensures a considerable improvement in the control quality. Figure 6 illustrates the control of the z variable, for which the changes were the most favourable.

The remaining responses of the quadcopter with constant and variable PID controllers parameters are presented in Figs. 7–9. Changes in individual PID controllers gains with gain scheduling are shown in Figs. 10–12.

Tab. 2. Control quality IAE for the different PID control systems

Controller	IAE e_1	IAE e_2	IAE e_3	IAE e_4	IAE e
Fixed gains	0.00542761	0.0244549	0.0293129	0.3711150	0.43031041
Fixed gains with filtration	0.00517794	0.0404676	0.0407506	0.2188910	0.30528714
Gain scheduling	0.00485863	0.0304711	0.0374924	0.1112040	0.18402613

IAE, integral absolute error; PID, proportional integral derivative

The developed control algorithm with a leading variable is simpler to implement than model-based adaptive methods. It is characterised by stability and accurate identification of the leading variable, which in this case is the quadcopter's mass. Based on the identified mass, the controller performs linear interpolation of the provided controller parameters from Tab. 1. Both the original parameters and the interpolated parameters were tested for stability.

The resistance of the control algorithm to external disturbances was evaluated by briefly applying an external force to the structure of the hovering quadcopter, thereby displacing it from its equilibrium position. Mass identification was solely based on the

DOI 10.2478/ama-2024-0004

dynamics equation for $\ddot{z}$ (41), resulting in a significantly simpler procedure than other adaptive algorithms that rely on a full model. Since the controller is based on stable and verified parameters regarding external disturbances, the control algorithm with a leading variable does not require additional on-line stability checks. This approach ensures the stability of the developed control system, which may not always be achievable in adaptive control systems based on full model identification.

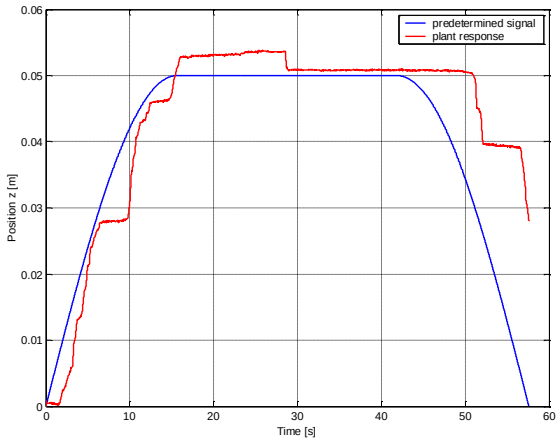

(a)

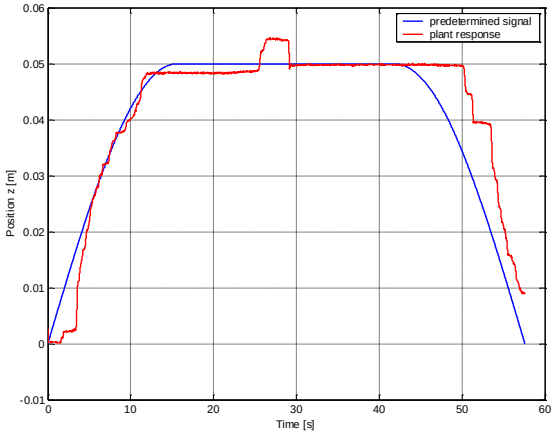

(b)

Fig. 6. Plant response for z: (a) PID controllers with fixed gains; (b) adaptive PID controllers with gain scheduling. PID, proportional integral derivative.

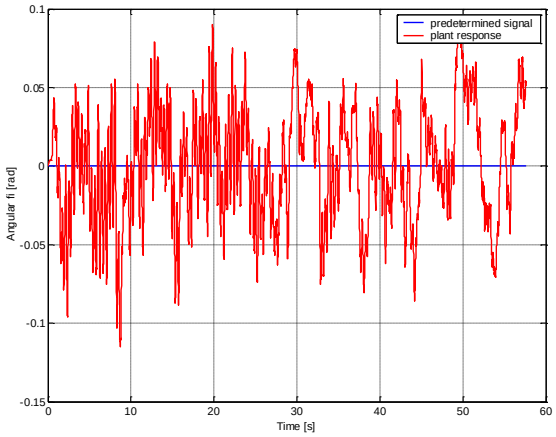

(a)

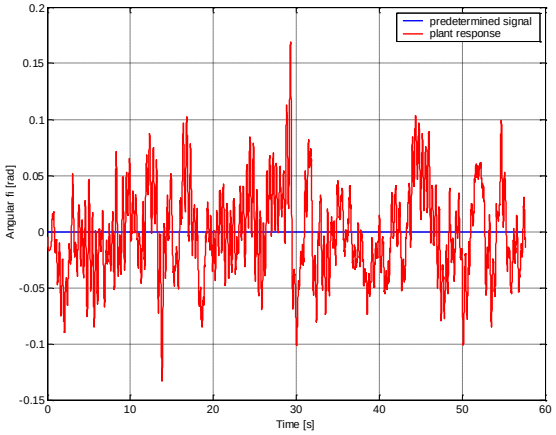

(b)

Fig. 7. Plant response for φ: (a) PID controllers with fixed gains; (b) adaptive PID controllers with gain scheduling. PID, proportional integral derivative.

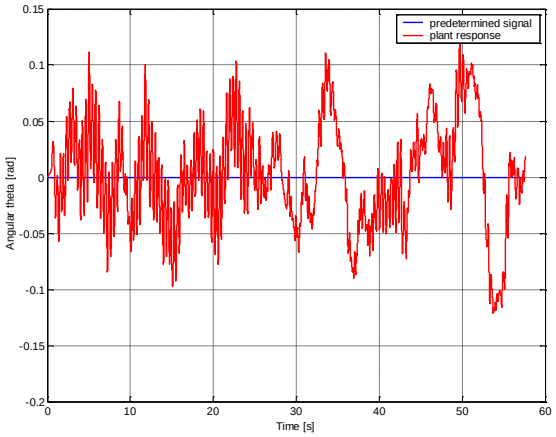

(a)

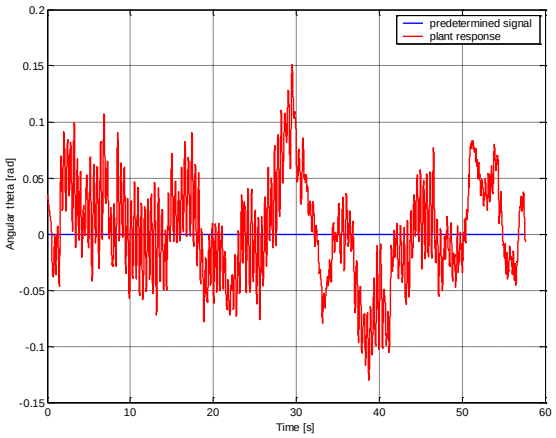

(b)

Fig. 8. Plant response for θ: (a) PID controllers with fixed gains; (b) adaptive PID controllers with gain scheduling. PID, proportional integral derivative.

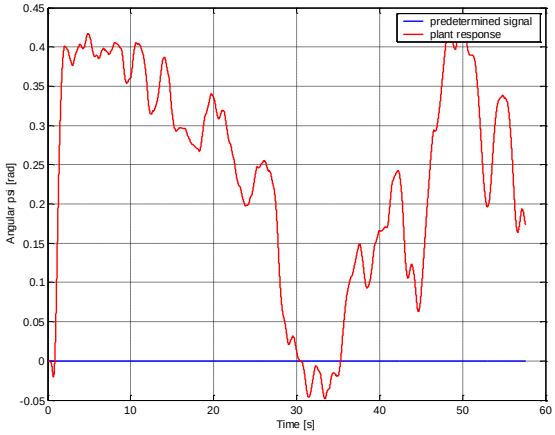

(a)

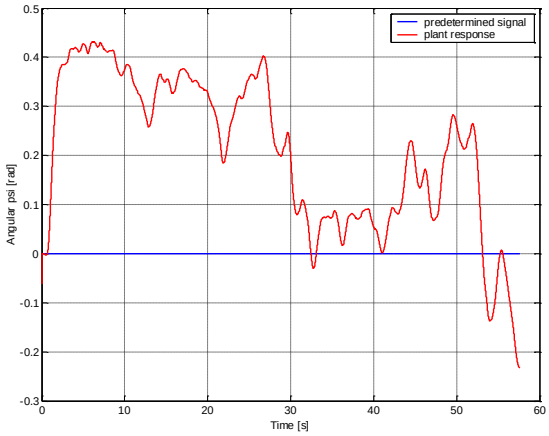

(b)

Fig. 9. Plant response for ψ: (a) PID controllers with fixed gains; (b) adaptive PID controllers with gain scheduling. PID, proportional integral derivative.

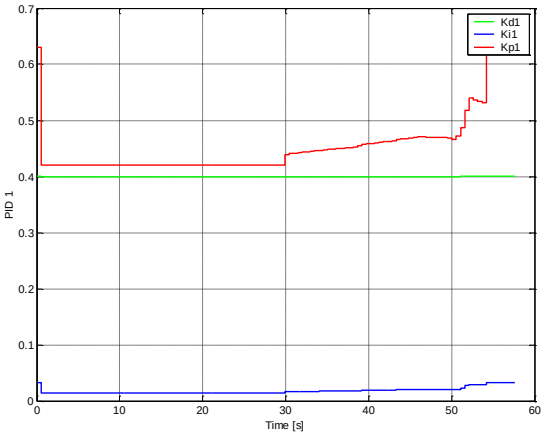

Fig. 10. Gains for adaptive PID 1 controllers with gain scheduling. PID, proportional integral derivative.

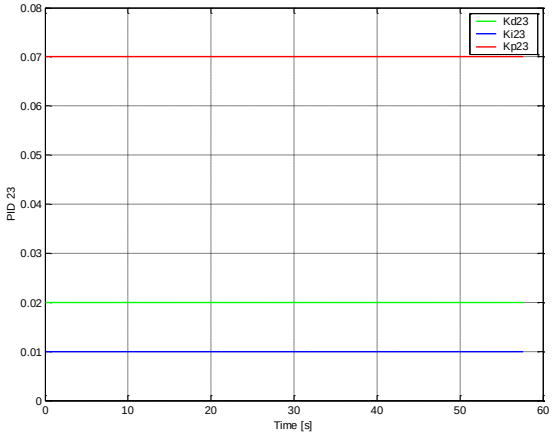

Fig. 11. Gains for adaptive PID 2 and PID 3 controllers with gain scheduling. PID, proportional integral derivative

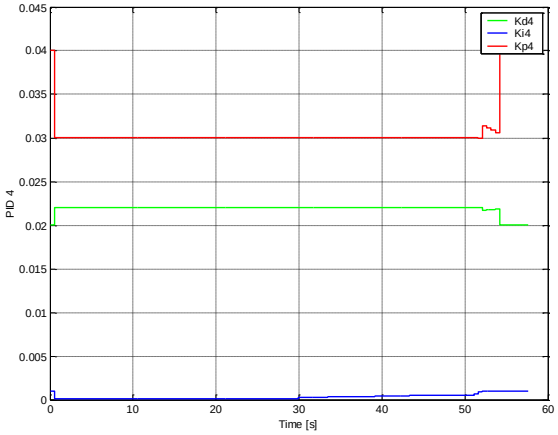

Fig. 12. Gains for adaptive PID 4 controllers with gain scheduling. PID, proportional integral derivative.

6. CONCLUSIONS

This article outlines quadcopter control experiments performed under laboratory conditions. The dynamic equations of motion derived for the plant were used to develop an accurate mass identification procedure; this required implementing the WRLS algorithm. The tests carried out for a real physical system confirmed that the use of low-pass and differential filters substantially improved the quality of the quadcopter control. The proposed adaptive PID control system with gain scheduling proved to be more suitable to control the response of a quadcopter with variable mass than classical PID controllers with fixed gains. The controllers with gain scheduling used setpoints determined through the optimisation procedure. The control system was stable irrespective of the quadcopter mass.

Despite significant measurement noise produced by the plant, the filter design process determines derivatives of signals with small errors. The use of PID controllers with fixed gains as well as low-pass and differential filters improved the plant response considerably. However, much higher control quality was observed for PID controllers with gain scheduling.

The identification procedure allows us to accurately estimate the quadcopter mass and, consequently, select the appropriate setpoints of the controllers (Fig. 5). The proposed control system

offers stable control of a quadcopter, it can be used with most commercially available controllers as it does not require high computational capacity.

The key advantage of the adaptation procedure with gain scheduling is that it allows the controller gains to vary depending on operating conditions (Figs. 10–12). This indicates that the controller can adapt to changes in plant dynamics and the operating environment. By adjusting the controller gains in RT, the controller can maintain stability and improve its tracking performance.

In contrast, other adaptation procedures, such as the adaptive control and model reference adaptive control, require controller gains to be adjusted based on the system's estimated parameters. This approach can be less effective as the estimated parameters may not accurately reflect plant dynamics or operating conditions.

Another advantage of gain scheduling is its ability to handle nonlinearities in plant dynamics (Figs. 6–9). Nonlinearities can cause the controller to behave unpredictably, leading to instability and poor performance. However, gain scheduling can account for these nonlinearities by adjusting the controller gains based on the specific operating conditions (Tab. 1).

Overall, the adaptation procedure with gain scheduling is a good method of control as it can adapt to changes in the plant dynamics and operating conditions, handle nonlinearities and provide excellent tracking performance.

The article discusses an adaptive PID control system developed to control a quadcopter. Based on the IAE index (Tab. 2), we can conclude that the developed gain scheduling control system achieves better results than the other tested control systems.

REFERENCES

1. Hasseni SEI, Abdou L, Glida HE. Parameters tuning of a quadrotor PID controllers by using nature-inspired algorithms. Evol Intel. 2021 Mar 1;14(1):61–73.
2. Khatoon S, Nasiruddin I, Shahid M. Design and Simulation of a Hybrid PD-ANFIS Controller for Attitude Tracking Control of a Quadrotor UAV. Arab J Sci Eng. 2017 Dec 1;42(12):5211–29.
3. Kuantama E, Vesselenyi T, Dzitac S, Tarca R. PID and Fuzzy-PID Control Model for Quadcopter Attitude with Disturbance Parameter. International Journal of Computers Communications & Control. 2017 Jun 29;12(4):519–32.
4. Rinaldi M, Primatesta S, Guglieri G. A Comparative Study for Control of Quadrotor UAVs. Applied Sciences. 2023 Jan;13(6):3464.
5. Burggräf P, Pérez Martínez AR, Roth H, Wagner J. Quadrotors in factory applications: design and implementation of the quadrotor's PID cascade control system. SN Appl Sci. 2019 Jun 14;1(7):722.
6. Abdelhay S, Zakriti A. Modeling of a Quadcopter Trajectory Tracking System Using PID Controller. Procedia Manufacturing. 2019 Jan 1;32:564–71.
7. Miranda-Colorado R, Aguilar LT. Robust PID control of quadrotors with power reduction analysis. ISA Transactions. 2020 Mar 1;98: 47–62.
8. Okyere E, Bousbaine A, Poyi GT, Joseph AK, Andrade JM. LQR controller design for quad-rotor helicopters. The Journal of Engineering. 2019;2019(17):4003–7.
9. Martins L, Cardeira C, Oliveira P. Linear Quadratic Regulator for Trajectory Tracking of a Quadrotor. IFAC-PapersOnLine. 2019 Jan 1;52(12):176–81.
10. Jia Z, Yu J, Mei Y, Chen Y, Shen Y, Ai X. Integral backstepping sliding mode control for quadrotor helicopter under external uncertain disturbances. Aerospace Science and Technology. 2017 Sep 1;68:299–307.
11. Xiu C, Liu F, Xu G. General model and improved global sliding mode control of the four-rotor aircraft. Proceedings of the Institution of Mechanical Engineers, Part I: Journal of Systems and Control Engineering. 2018 Apr 1;232(4):383–9.
12. Mofid O, Mobayen S. Adaptive sliding mode control for finite-time stability of quad-rotor UAVs with parametric uncertainties. ISA Transactions. 2018 Jan 1;72:1–14.
13. Castillo-Zamora JJ, Camarillo-GóMez KA, PéRez-Soto GI, RodríGuez-ReséNdiz J. Comparison of PD, PID and Sliding-Mode Position Controllers for V–Tail Quadcopter Stability. IEEE Access. 2018;6:38086–96.
14. Liu H, Tu H, Huang S, Zheng X. Adaptive Predefined-Time Sliding Mode Control for QUADROTOR Formation with Obstacle and Inter-Quadrotor Avoidance. Sensors. 2023 Jan;23(5):2392.
15. Jiang F, Pourpanah F, Hao Q. Design, Implementation, and Evaluation of a Neural-Network-Based Quadcopter UAV System. IEEE Transactions on Industrial Electronics. 2020 Mar;67(3):2076–85.
16. El Gmili N, Mjahed M, El Kari A, Ayad H. Particle Swarm Optimization and Cuckoo Search-Based Approaches for Quadrotor Control and Trajectory Tracking. Applied Sciences. 2019 Jan;9(8):1719.
17. Tanveer MH, Ahmed SF, Hazry D, Warsi FA, Joyo MK. Stabilized Controller Design for Attitude and Altitude Controlling of Quad-Rotor Under Disturbance and Noisy Conditions. AJAS. 2013 Jul 24;10(8):819–31.
18. Moreno-Valenzuela J, Pérez-Alcocer R, Guerrero-Medina M, Dzul A. Nonlinear PID-Type Controller for Quadrotor Trajectory Tracking. IEEE/ASME Transactions on Mechatronics. 2018 Oct;23(5):2436–47.
19. Wu Y, Hu K, Sun XM. Modeling and Control Design for Quadrotors: A Controlled Hamiltonian Systems Approach. IEEE Transactions on Vehicular Technology. 2018 Dec;67(12):11365–76.
20. Kidambi KB, Tiwari M, Ijoga EO, MacKunis W. Adaptive Modified RISE-based Quadrotor Trajectory Tracking with Actuator Uncertainty Compensation [Internet]. arXiv; 2023 [cited 2023 Dec 8]. Available from: http://arxiv.org/abs/2303.10270
21. Dong T, Zhang Y, Liu Y, Chen C. Quantitative Study of Load Stability of Quadrotor Based on Lyapunov Exponents. International Journal of Antennas and Propagation. 2023 Apr 19;2023:e9918890.
22. Tal E, Karaman S. Accurate Tracking of Aggressive Quadrotor Trajectories Using Incremental Nonlinear Dynamic Inversion and Differential Flatness. IEEE Transactions on Control Systems Technology. 2021 May;29(3):1203–18.
23. Hong JY, Chiu PJ, Pong CD, Lan CY. Attitude and Altitude Control Design and Implementation of Quadrotor Using NI myRIO. Electronics. 2023 Jan;12(7):1526.
24. Niederliński A, Mościński J, Ogonowski Z. AdaptiveControl. PWN. Warsaw. 1995.
25. Audronis T. Building Multicopter Video Drones. Packt Publishing; 2014.
26. Bouabdallah S, Noth A, Siegwart R. PID vs LQ control techniques applied to an indoor micro quadrotor. In: 2004 IEEE/RSJ International Conference on Intelligent Robots and Systems (IROS) (IEEE Cat No04CH37566) [Internet]. 2004 [cited 2023 Dec 8]. p. 2451–6 vol.3.
27. Janecki D. Globally stable and exponentially convergent adaptive control. International Journal of Control. 1986 Feb 1;43(2):601–13.
28. Ammar NB, Gue SB, Ge JH. Modeling and Sliding Mode Control of a Quadrotor Unmanned Aerial Vehicle. 3rd International Conference on Automation, Control, Engineering and Computer Science. 2016: 834-840.
29. Herrera M, Chamorro W, Gómez AP, Camacho O. Sliding Mode Control: An Approach to Control a Quadrotor. In: 2015 Asia-Pacific Conference on Computer Aided System Engineering [Internet]. 2015 [cited 2023 Dec 8]. p. 314–9.
30. Rabhi A, Chadli M, Pegard C. Robust fuzzy control for stabilization of a quadrotor. 15th International Conference on Advanced Robotics (ICAR). 2011 Jun 1: 471-475.
31. Szcześniak A, Szcześniak Z. Algorithmic Method for the Design of Sequential Circuits with the Use of Logic Elements. Applied Sciences. 2021 Jan;11(23):11100.

32. Jacobsen RH, Matlekovic L, Shi L, Malle N, Ayoub N, Hageman K, et al. Design of an Autonomous Cooperative Drone Swarm for Inspections of Safety Critical Infrastructure. Applied Sciences. 2023 Jan;13(3):1256.
33. Cheng LL, Liu HB. Examples of quadrocopter control on ROS. In: 2015 IEEE 9th International Conference on Anti-counterfeiting, Security, and Identification (ASID) [Internet]. 2015 [cited 2023 Dec 8]. p. 92–6.
34. Florek M, Huba M, Duchoň F, Šovčík J, Kajan M. Comparing approaches to quadrocopter control. In: 2014 23rd International Conference on Robotics in Alpe-Adria-Danube Region (RAAD) [Internet]. 2014 [cited 2023 Dec 8]. 1–6.
35. Holonec R, Copindean R, Dragan F, Rápolti L. Self-guided AR Drone using LabVIEW. 2016;57(5).
36. Gardecki S, Giernacki W, Goslinski J, Kasinski A. An adequate mathematical model of four-rotor flying robot in the context of control simulations. Journal of Automation Mobile Robotics and Intelligent Systems [Internet]. 2014 [cited 2023 Dec 8];Vol. 8, No. 2.
37. Koruba Z, Control and correction of a gyroscopic platform mounted in a flying object. Journal of Theoretical and Applied Mechanics. 2007. vol. 45, no. 1, p.41–51
38. Koruba Z, Dziopa Z, Krzysztofik I. Dynamics and control of a gyroscope-stabilized platform in a self-propelled anti-aircraft system. Journal of Theoretical and Applied Mechanics. 2010;48(1):5–26.
39. Astrom K, Wittenmark B, Adaptive control, Addison-Wesley Publishing Company, 1989.
40. Formánek I, Farana R. Experimental identification of mechanical properties of variable speed drives. In: 2017 18th International Carpathian Control Conference (ICCC) [Internet]. 2017 [cited 2023 Dec 8]. 117–22.
41. Formánek I, Farana R. Design and synthesis of control systems of material flow in industrial companies. In: 2017 18th International Carpathian Control Conference (ICCC) [Internet]. 2017 [cited 2023 Dec 8]. 112–6.
42. Viteckova M, Vitecek A, Janacova D. Robust stability and desired model method. In: 2018 Cybernetics & Informatics (K&I) [Internet]. 2018 [cited 2023 Dec 8]. 1–5.
43. Viteckova M, Vitecek A, Sladka K. Controller tuning by desired model method. In: 2017 18th International Carpathian Control Conference (ICCC) [Internet]. 2017 [cited 2023 Dec 8]. 171–6.
44. Viteckova M, Vitecek A. 2DOF PID controller tuning for integrating plants. In: 2016 17th International Carpathian Control Conference (ICCC) [Internet]. 2016 [cited 2023 Dec 8]. 793–7.
45. Janecki D. New recursive parameter estimation algorithms with varying but bounded gain matrix. International Journal of Control. 1988 Jan 1;47(1):75–84.
46. Basri A, Husain A, A. Danapalasingam K. Nonlinear Control of an Autonomous Quadrotor Unmanned Aerial Vehicle using Backstepping Controller Optimized by Particle Swarm Optimization. Journal of Engineering Science and Technology Review. 2015 Sep 1;8:39–45.
47. Erkol HO. Attitude controller optimization of four-rotor unmanned air vehicle. International Journal of Micro Air Vehicles. 2018 Mar 1;10(1):42–9.
48. Goldberg DE, Holland JH. Genetic Algorithms and Machine Learning. Machine Learning. 1988 Oct 1;3(2):95–9.
49. Chandra Mohan B, Baskaran R. A survey: Ant Colony Optimization based recent research and implementation on several engineering domain. Expert Systems with Applications. 2012 Mar 1;39(4): 4618–27.
50. Karaboga D, Gorkemli B, Ozturk C, Karaboga N. A comprehensive survey: artificial bee colony (ABC) algorithm and applications. Artif Intell Rev. 2014 Jun 1;42(1):21–57.
51. El Gmili N, Mjahed M, El Kari A, Ayad H. Particle Swarm Optimization and Cuckoo Search-Based Approaches for Quadrotor Control and Trajectory Tracking. Applied Sciences. 2019 Jan; 9(8):1719.
52. Joshi AS, Kulkarni O, Kakandikar GM, Nandedkar VM. Cuckoo Search Optimization- A Review. Materials Today: Proceedings. 2017 Jan 1;4(8):7262–9.
53. Imane S, Mostafa M, Hassan A, Abdeljalil EK. Control of a quadcopter using reference model and genetic algorithm methods. In: 2015 Third World Conference on Complex Systems (WCCS) [Internet]. 2015 [cited 2023 Dec 8]. p. 1–6.
54. LabVIEW™ . System Identification Toolkit Algorithm References. ni.com. June 2008.
55. Cedro L, Janecki D., Determining of Signal Derivatives in Identification Problems -FIR Differential Filters, Acta Montanistica Slovaca, R 16, ISSN 1335-1788, 47-54, 2011.
56. Cedro L, Filtry różniczkujące w układach czasu rzeczywistego, Przegląd Elektrotechniczny, ISSN 0033-2097, R. 89 NR 7/2013. 137-141.

Leszek Cedro: https://orcid.org/0000-0002-2419-4044

Krzysztof Wieczorkowski: https://orcid.org/0009-0008-8074-8284

Adam Szcześniak: https://orcid.org/0000-0003-2411-9279